GPS Solutions (2023) 27:91
https://doi.org/10.1007/s10291-023-01433-5

ORIGINAL ARTICLE

Investigation into the nonlinear Kalman filter to correct the INS/GNSS integrated navigation system

Konstantin Neusypin[1] · Andrey Kupriyanov[2] · Andrey Maslennikov[1] · Maria Selezneva[1]

Received: 7 November 2021 / Accepted: 28 February 2023

Abstract
The integrated navigation system is the inertial navigation system (INS), corrected by global navigation satellite system (GNSS) data. The correction could be done algorithmically by utilizing nonlinear Kalman filtering (NKF). In practice, the NKF uses an INS error model as an a priori model that is not always adequate to handle the dynamics of the true and unknown INS error model. To eliminate such modeling errors, we propose a new INS/GPS correction approach with modified adaptive NKF. In the proposed NKF, instead of the a priori model, the model constructed during the pre-flight test for a particular INS is used. To realize this, the full algorithm includes an INS error model construction algorithm, a way of reduced measurement generation, and criteria for divergence detection. INS error model construction both during pre-flight test and during flight is done by the group method of data handling (GMDH). Flight experiments were performed for an empirical study of the INS error model and its effect on the total accuracy of computed navigational data. The navigational equipment was installed on the balloon—an airborne radio-transparent object. The results of the experiments validate the effectiveness and accuracy of the proposed INS/GPS correction approach.

Keywords Inertial navigation systems · GNSS · Nonlinear Kalman filter · Error model · Adaptation · Group method of data handling · GPStation6 · RTK · SPAN

Introduction

The accurate determination of the spatial location and temporal relation of objects is essential in many applications. INS and GNSS applications are widespread, particularly in aviation (Proletarsky et al. 2019; Selezneva et al. 2019). The increasing accuracy of aircraft navigation measurements is typically achieved via correction algorithms. Usually, for INS correction, various estimation algorithms are applied, for example, a nonlinear Kalman filter (Zheng et al. 2018, Simon 2006; Julier and Uhlmann 1997). In NKF, an INS error model is used, and the estimation accuracy depends on the reliability of such a model. To create reliable and adequate model, the ideas of the federated Kalman filter (Ali and Jiancheng 2005; Yang et al. 2020) and the model construction were used (Fantinutto et al. 2005; Kondo 1998). An evolutionary algorithm may also be used for this purpose. However, such an approach requires additional time to select or construct a model and needs a good performance of the onboard computer.

We propose constructing the INS error model during preliminary pre-flight tests and then using it inside the adaptive version of the NKF. The advantage of this approach is the ability to use the error model of a specific INS with its own characteristics. During the INS operation, the error dynamics will be slightly different, but its model will retain the individual characteristics of that particular INS. Therefore, studying these characteristics and their impact on the INS error model and, finally, on the accuracy of navigational data is an actual problem.

✉ Maria Selezneva
ms.selezneva@bmstu.ru

Konstantin Neusypin
neysipin@mail.ru

Andrey Kupriyanov
aoku28@gmail.com

Andrey Maslennikov
amas@bmstu.ru

[1] Bauman Moscow State Technical University, Moscow, Russia

[2] Moscow State University of Geodesy and Cartography, Moscow, Russia

Published online: 21 March 2023

The proposed algorithm verification must be carried out by analyzing the data of flight experiments. For this purpose, a mathematical modeling approach is applied. It involves using the a priori INS error model and GNSS error data usually represented by the white noise stochastic process (George and Sukkarieh 2005; Gao et al. 2006). The actual INS error dynamics depend on the INS type, individual characteristics, and specific environmental conditions. Therefore, the real situation in flight is different from the test models. To deal with that we used the results from flight experiments in our studies.

First, two NKF implementation methods, often used in INS correction, are presented. Then, we describe the GMDH (group method of data handling) algorithm used to construct the INS error model based on a measurement sample as a difference between the INS and GNSS data obtained in flight, followed by presenting a scalar criterion as an indicator of the non-measured state components of the estimation process convergence. We propose a new INS correction scheme as an algorithm using actual measurements and modified adaptive NKF realization. The subsequent sections describe the experimental setup and provide the results of the experiments and corresponding discussions.

NKF implementation methods

In practice, strict requirements are imposed on the navigational data accuracy; therefore, the integration of the INS with GNSS and the subsequent information processing uses the NKF (Simon 2006; Carvalho et al. 1997). Suppose the equation for the state vector of the INS error model has the form:

$$x_k = F_k\left(x_{k-1}\right) + w_k \tag{1}$$

where x_k is the state vector, $F_k\left(x_{k-1}\right)$ denotes the nonlinear vector function, w_k is the input noise vector. The measurement equation is the following,

$$z_k = H_k x_k + v_k \tag{2}$$

where z_k is the measurement vector, H_k is the measurement matrix, v_k is the measurement noise vector, w_k and v_k are two uncorrelated discrete random processes similar to Gaussian white noise processes with zero mean and covariance matrices Q_k and R_k, respectively. The NKF equations take the form:

$$\begin{aligned}
\hat{x}_k &= \hat{x}_{k|k-1} + K_k(\hat{x}_{k-1})[z_k - H_k\hat{x}_{k|k-1}] \\
\hat{x}_{k|k-1} &= F_k(\hat{x}_{k-1}) \\
K_k(\hat{x}_{k-1}) &= P_{k|k-1}H_k^T[H_kP_{k|k-1}H_k^T + R_k]^{-1} \\
P_{k|k-1} &= \frac{\partial F_k(\hat{x}_{k-1})}{\partial x_{k-1}^T}P_{k-1}\left[\frac{\partial F_k(\hat{x}_{k-1})}{\partial x_{k-1}^T}\right]^T + Q_k \\
P_k &= \left[I - K_k(\hat{x}_{k-1})H_k\right]P_{k|k-1}
\end{aligned} \tag{3}$$

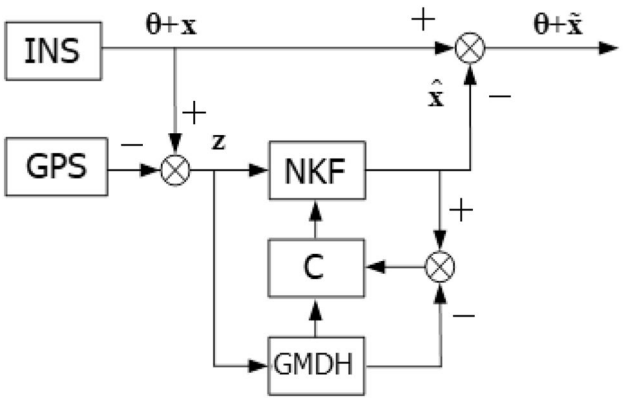

Fig. 1 INS correction scheme using the group method of data handling. INS is the inertial navigation system, GPS is the receiver, NKF denotes the nonlinear Kalman filter, GMDH stands for group method of data handling, C is a criterion to indicate the divergence of the estimate process (Selezneva and Neusypin 2016), θ is the navigation information, x is the INS errors vector, z is the measurement vector, $\hat{x}$ is the estimated vector, and $\tilde{x}$ is the vector of the estimation errors

where I denoted the identity matrix and P_k is the covariance matrix of estimation errors.

This type of NKF is applicable only when the posterior probability density is unimodal. However, when the posterior probability density is multimodal, then the estimation algorithm should use a set of delta functions representing that posterior probability density.

There also exist approaches where the implementations of the NKF are reduced to solving a stochastic partial differential equation written in the Ito or the Stratonovich form. However, such implementations require applying special integration rules that do not coincide with the usual ones, resulting in increased numerical operations and computational complexity.

It is possible to consider all aspects of the INS error dynamics, especially in the case of specific INS and environmental conditions in flight. For instance, this could be done by constructing a nonlinear INS error model using one of the evolutionary algorithms (Fantinutto et al. 2005; Kondo 1998).

The constructed nonlinear model is further used as a reference model to ensure the adequacy of the NKF model and the real INS error dynamics. The diagram of the INS correction using the group method of data handling is shown in Fig. 1 (Song and Wang 2017, Yin et al. 2019).

Data from the INS and GNSS are jointly processed. First, the difference between INS and GNSS data is computed, yielding a mixture of INS and GNSS errors. Further, the mixture of errors z is processed using the NKF, and the computed estimate is fed to the output of the INS correction scheme. At the same time, the INS error model is constructed using the measurements by the GMDH algorithm.

The INS errors obtained through the GMDH algorithm are compared with the estimated ones. Further, if the criterion on block C is satisfied, that implies that the estimation process diverges, then the constructed INS error model replaces the one in the NKF.

Let us briefly discuss the GMDH algorithm. The first stage compares the predefined basic functions with the measurement sample. The best functions are selected based on selection criteria. At the next stage, the selected functions are crossed, and model candidates are formed, which are again subjected to selection criteria. As a result of such an iterative process, the error model is obtained. It is necessary to note that the criterion of the estimation process divergence must be included in the structure of the NKF.

Let us consider another way of NKF implementation. The state equation of the estimating process x has the form

$$x_k = f(x_{k-1}, \xi_{k-1}) \tag{4}$$

where ξ is the input noise and $f(\cdot)$ denotes the well-known nonlinear vector function. The a priori probability density of vector x is $p_{\text{ap}}(x_0)$. The measurement equation has the following form:

$$y_k = S(x_k, n_k) \tag{5}$$

where n is the measurement noise, and $S(\cdot)$ is the nonlinear vector function. Vector y includes INS and GNSS data as well as measurements of pseudoranges and pseudo velocities computed in the GNSS receiver.

The optimal filtering is based on the theory of statistical solutions of the Stratonovich equation (Kurtz et al. 1995; Chechkin and pavlyukevich 2014). The following Stratonovich equation describes the change in the posterior probability density:

$$\begin{aligned} p\left(x_k \middle| \mathrm{Y}_0^k\right) &= c\, p\left|\left(y_k \middle| x_k\right)\right. \\ &\int_{-\infty}^{\infty} p\left(x_{k-1} \middle| \mathrm{Y}_0^{k-1}\right) p\left(x_k \middle| x_{k-1}\right) \mathrm{d}x_{k-1}, p\left(x_0 \middle| \mathrm{Y}_0^0\right) \\ &= p_{ap}\left(x_0\right) \end{aligned} \tag{6}$$

where c is the normalization constant, $Y_0^k = \left|y_1, y_1 \ldots y_k\right|$ are measurements, $p\left(y_k | x_k\right)$ denotes the one-step likelihood function, $p\left(x_{k-1} | Y_0^{k-1}\right)$ denotes the posterior probability density, and $p\left(x_k | x_{k-1}\right)$ denotes the transition probability density of the Markov process, determined by the stochastic model of this process (4).

In practice, the solution of the Stratonovich equation is an extended Kalman filter (EKF) (Wan and Nelson 2001; Lee and Ricker 1994). The EKF is the recurrent algorithm for estimating $\hat{x}_k$ and the error covariance $D_{x,k}$. The EKF is much easier to implement than numerically solving the Stratonovich equation in a computer system.

The EKF algorithm consists of two stages: prediction and update. During the first stage, the prediction (extrapolation) of the state vector is computed using the following expression

$$\tilde{x}_k = f_{k-1}(\hat{x}_{k-1}) \tag{7}$$

where $f_{k-1}\left(\hat{x}_{k-1}\right)$ for each component of x is determined separately. The variance matrix D is computed as follows

$$\tilde{D}_{x,k} = \frac{\partial f_{k-1}\left(x_{k-1}\right)}{\partial x_{k-1}} D_{x,k-1} \left(\frac{\partial f_{k-1}\left(x_{k-1}\right)}{\partial x_{k-1}}\right)^T + g_{k-1}\left(x_{k-1}\right) D_\zeta\, g_{k-1}^T\left(x_{k-1}\right) \tag{8}$$

During the second stage, the corresponding updates for the predicted state vector and its covariance are computed through the following set of equations:

$$\begin{aligned} K_k &= \tilde{D}_{x,k} \left(\frac{\partial S_k\left(c\tilde{x}_k\right)}{\partial x_{k-1}}\right)^T \left(\frac{\partial S_k\left(c\tilde{x}_k\right)}{\partial x_{k-1}} \tilde{D}_{x,k} \left(\frac{\partial S_k\left(c\tilde{x}_k\right)}{\partial x_{k-1}}\right)^T + D_n\right)^{-1} \\ D_{x,k} &= \left(I - K_k \frac{\partial S_k\left(c\tilde{x}_k\right)}{\partial x_{k-1}}\right) \tilde{E}_k \\ \hat{x}_k &= \tilde{x}_k + K_k\left(y_k - S_k\left(c\tilde{x}_k\right)\right) \end{aligned} \tag{9}$$

The two ways of NKF implementation were presented. The first way, shown in Fig. 1, is used in the correction scheme, for instance, for a maneuverable aircraft, since it could adapt the model. The second one could be used for an aircraft with low-speed dynamics, for instance, transport aircraft. The advantage of the second one is the much simpler realization on the onboard computer. It also has satisfactory accuracy of the estimates with a good choice of the INS error model (Shen et al. 2016; Neusypin et al. 2018). The comparison of those two NKF implementations will be shown later based on the experimental data obtained in flight.

Group method of data handling

The GMDH approach for constructing models assumes that information that characterizes the dynamics of an object of interest is contained in measurements (represented as an observation table or a set of data samples) Ivakhnenko (1970). This approach uses a criteria ensemble for model selection from a set of candidates. Moreover, it does not require any a priori identification of the object regularities. To construct a mathematical model in such a way, we must specify the selection criteria for model selection. Eventually, the model with optimal complexity, determined by these

criteria, is selected automatically. The minimum value of the selection criteria determines the adequacy of the constructed model. The right choice of selection criterion allows to exclude unneeded, random, and non-informative state variables and to determine their interrelation in an optimal way. According to Leibniz, "if half of the art of the inventor consists in gradually increasing the complexity of combinations (or in building a generator of sentences), then it can be argued that the second half is in the selection of selection criteria" (Selezneva et al. 2017).

The selection criteria make the choice of the model unambiguous. In GMDH, all optimization issues are efficiently solved by numerical algorithms only based on given training and test data sets. No information on the probability distribution is needed. As a threshold self-selection, various heuristic criteria are consistently used: correlation coefficient, the criterion for convergence of arguments, the criterion of matrix condition, and, mainly, the minimum mean squared error (MMSE) criterion (Csorgo et al. 1981; Rao 1980).

Basic principles for designing GMDH algorithms.

A full description of an object could be formalized as follows

$$\Phi = f_1(x_1, x_2, x_3, ..., x_i) \tag{10}$$

and should be replaced with multiple private descriptions:

$$y_1 = f_1(x_1, x_2), \quad y_2 = f_1(x_1, x_3), \quad \dots \quad y_m = f_1(x_{n-1}, x_n) \tag{11}$$

$$z_1 = f_1(y_1, y_2), \quad z_2 = f_1(y_1, y_3), \quad \dots, \quad z_p = f_1(y_{m-1}, y_m) \tag{12}$$

where $m = C_n^2$, $p = C_m^2$ and so on. The GMDH algorithms must then satisfy the following two conditions:

1. The function $f_1(\cdot)$ is the same in all equations. Eliminating the intermediate variables makes it possible to obtain an "analog" of the full description.
2. The analog must correspond to the full description. By comparing the analog and the actual complete description in its general form, one can find equations for constructing the coefficients of the complete description.

When these conditions are satisfied, GMDH makes it possible to find estimates for the coefficients of the complete equation, even if their number is large. To be able to reuse the data in the algorithm, it is necessary to solve the interpolation problem up to the end at each level of the multi-row system. All GMDH algorithms have this property. In GMDH, the rule of threshold self-selection is used as well as the idea of selection during the compilation of mathematical algorithms (Shen et al. 2016; Ivakhnenko 1971). This led to the fact that ineffective combinations discarded in the first rows of self-selection cannot provide optimal combinations of the next row if they were skipped further. The GMDH algorithm diagram is presented in Fig. 2.

Let us now present the application of GMDH for the INS error model construction. The measurements are formed using the difference between the INS and GNSS data. The constructing model using the GMDH algorithm looks like

$$y_1(\mathrm{d}V) = b_{01} + b_{11}x_1 + b_{21}x_3 + b_{31}x_1^2 + b_{41}x_3^2 + b_{51}x_1x_3 \tag{13}$$

$$y_3(e) = b_{03} + b_{13}x_3 + b_{23}x_4 + b_{33}x_3^2 + b_{43}x_4^2 + b_{54}x_3x_4 \tag{14}$$

where the estimated coefficients are

$$b_{01} = 5.86; b_{11} = -3.27; b_{21} = 4.21; \; b_{31} = 0.0013;$$
$$b_{41} = -0.0804; \; b_{51} = 0.08$$

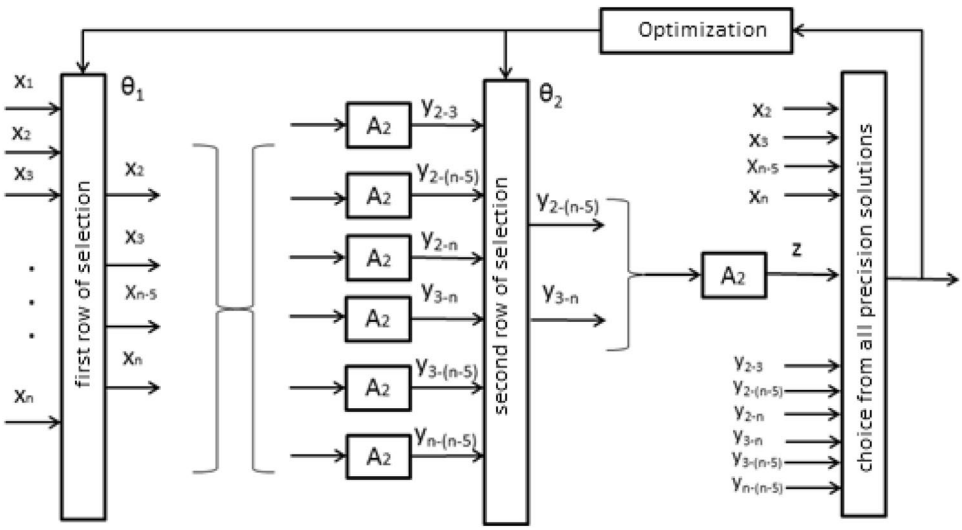

Fig. 2 Diagram representing the general idea of the GMDH algorithm. After the first and second rows of selection, the choice from all precision solutions is made, and the optimization is performed. Optimization results are then used in the first row of selection

These equations are obtained with the help of the GMDH algorithm using real measurements obtained during the flight experiment. The presented model is used in the NKF as a system model, i.e., the INS error model. Thus, the INS error model of a particular INS during the current flight experiment has been obtained. The efficiency of using such an INS error model in the NKF using data sets from flight experiments will be shown later.

In the INS correction scheme, the Rao–Cramer inequality can be used as an indicator of estimation process convergence (Belavkin 2013; Trees and Bell 2007; Tichavsky et al. 1998; Simandl et al. 2001). The well-known criterion has the following matrix form

$$v_k v_k^T \le \gamma H_k P_{k|k-1} H_k^T + R_k \tag{15}$$

or in a scalar form

$$v_k^2 \le \gamma P_{k|k-1} + r_k \tag{16}$$

Here γ is a coefficient put in for practical reasons, and it determines the level of covariance permissible values, above which the estimation process is considered divergent. However, during model construction by the GMDH algorithm, this criterion is applicable only for directly measured state variables. In the case of a reduced one, when not all states are directly measured, the formulation of the criterion could be done as described below.

Formation of reduced measurements for directly unmeasured state variables

We use a nonlinear INS error model, obtained with the help of GMDH, to generate measurements directly of not measured state variables. The divergence criterion r contains the variance of the reduced noise that must be determined. The estimate of x_1 with the scalar measurement of z can be formulated as:

$$x_1 = \begin{bmatrix} H \\ H\Phi \\ \cdots \\ \cdots \\ H\Phi^{n-1} \end{bmatrix}^{-1} \left\{ \begin{bmatrix} z_1 \\ z_2 \\ \cdots \\ \cdots \\ z_n \end{bmatrix} - \begin{bmatrix} v_1 \\ Hw_1 + v_2 \\ H\Phi w_1 + Hw_2 + v_3 \\ \cdots \\ H\Phi^{n-2} w_1 + \cdots + v_n \end{bmatrix} \right\} \tag{17}$$

The measurement equation for the $(n+1)^{th}$ moment has the form

$$z_{n+1} = Hx_{n+1} + v_{n+1} \tag{18}$$

The state $x_n + 1$ in terms of its value at time moment $n+1$ can be expressed as follows:

$$x_{n+1} = \Phi^n x_1 + \Phi^{n-1} w_1 + \ldots + w_n \tag{19}$$

and substituting the expression for $x_n + 1$ into the measurement equation z_{n+1}, one can obtain

$$z_{n+1} = H\Phi^n x_1 + H\Phi^{n-1} w_1 + \ldots + Hw_n + v_{n+1} \tag{20}$$

and then substitute in this equation the expression for x_1, one can get

$$\begin{aligned} z_{n+1} =& H\Phi^n \begin{bmatrix} H \\ H\Phi \\ \ldots \\ \ldots \\ H\Phi^{n-1} \end{bmatrix}^{-1} \begin{bmatrix} z_1 \\ z_2 \\ \ldots \\ \ldots \\ z_n \end{bmatrix} \\ & - H\Phi^n \begin{bmatrix} H \\ H\Phi \\ \ldots \\ \ldots \\ H\Phi^{n-1} \end{bmatrix}^{-1} \begin{bmatrix} v_1 \\ Hw_1 + v_2 \\ H\Phi w_1 + Hw_2 + v_3 \\ \ldots \\ H\Phi^{n-2} w_1 + \ldots + v_n \end{bmatrix} \\ & + H\Phi^{n-1} w_1 + H\Phi^{n-2} w_2 + \ldots + Hw_n + v_{n+1} \end{aligned} \tag{21}$$

The last equation reformulates the measurement equations in terms of the noise variables.

Let us introduce the notation:

$$\begin{bmatrix} a_1 & a_2 & \cdots & a_n \end{bmatrix} = H\Phi^n \begin{bmatrix} H \\ H\Phi \\ \cdots \\ \cdots \\ H\Phi^{n-1} \end{bmatrix}^{-1} \tag{22}$$

$$z^*_{k(n+1)} = \begin{bmatrix} a_1 & a_2 & \cdots & a_n \end{bmatrix} \begin{bmatrix} z_1 \\ z_2 \\ \vdots \\ z_n \end{bmatrix}_k \tag{23}$$

$$\begin{aligned} v_0^1 &= b_1 w_1 + b_2 w_2 + \ldots + b_n w_n - a_1 v_1 + a_2 v_2 - \ldots - a_n v_n + v_{n+1} \\ &= H\Phi^n \begin{bmatrix} H \\ H\Phi \\ \ldots \\ \ldots \\ H\Phi^{n-1} \end{bmatrix}^{-1} \begin{bmatrix} v_1 \\ Hw_1 + v_2 \\ H\Phi w_1 + Hw_2 + v_3 \\ \ldots \\ H\Phi^{n-2} w_1 + \ldots + v_n \end{bmatrix} \end{aligned} \tag{24}$$

where v_1^0 denotes the reduced measurement noise. With (24), it is possible to estimate the reduced measurement noise level for each vector component x. The variance of the reduced measurement noise is used in the divergence criterion (15). A diagram with this criterion is shown in Fig. 3. In the BGRM block, the reduced measurements are computed according to (21). Eventually, after a sequence of

n measurements (*n* measurement sub-ticks), we can directly estimate the entire vector *x*.

The proposed adaptive NKF operates as follows. First, the difference between the INS and GNSS measurements is calculated (the signals are synchronized). Then, a mixture of INS and GNSS errors is passed to the input of the NFK and to the input of the Measurement Formation Block (MFB) (measurements are collected to a data set). After the MFB, the signal is sent to the GMDH for building INS error models. The INS error from the GMDH block is compared with the one from the NKF estimate. If the error difference exceeds the predefined value in the K block, then the GMDH model is used in the NKF instead of the a priori computed model. If the error difference does not exceed the threshold, then the NKF operates with an a priori computed model. The estimate from the NKF is fed into the output signal of the INS to compensate for the INS error. The diagram of the described algorithm is presented in Fig. 4.

Experimental research

A wide range of motion of a balloon provides a unique opportunity to use multisystem multifrequency orbital information (including from sub-horizon satellites) to study the radio navigational field and subtle effects of inertial navigation (Selezneva et al. 2017) and gravimetry. We used a multifunctional autonomous measurement system (MAMS) to collect different navigational data during the flight experiment. The MAMS allows to collect data from GNSS from 6 independent receivers, INS data, and ionospheric data in real time. The autonomous operation time of MAMS is about 4–6 h, and the working temperature range is from − 30 to + 60 °C. The MAMS equipment is shown in Fig. 5.

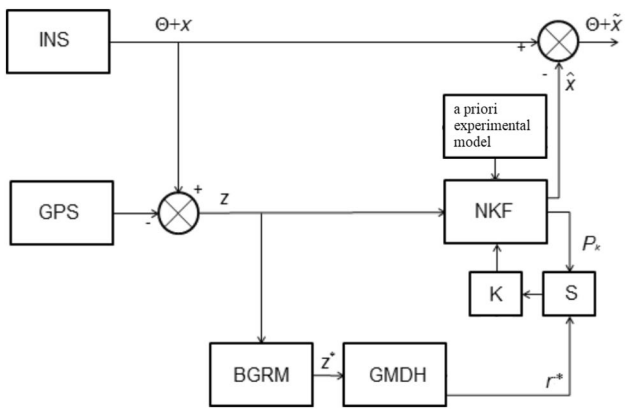

Fig. 3 A functional diagram with scalar criterion, where BGRM is the block for generating reduced measurements, S is the divergence criterion, and K is the key

The balloon was equipped with rigidly mounted INS and GNSS devices, a fiber-optic gyroscopic system with NovAtel SPAN-CPT accelerometers, as well as several GNSS receivers from Russian domestic producers. These receivers, smart antennas, and base stations operate on all frequencies of GLONASS, GPS, BDS, Galileo, and wide-range GNSS augmentation.

The advantages and the uniqueness of the experiment of the balloon are that its dome is radio transparent (radio signals are passed through the dome undistorted), and its movements are smooth and depend on the wind speed in different layers of the atmosphere. In addition, its load and, consequently, the whole equipment is almost free from mechanical vibrations in comparison with other carriers. It must be noted that the vertical balloon position is possible to control. The pre-flight assembly of MAMS is presented in Fig. 6. The general diagram of a multifunctional autonomous measurement system is shown in Fig. 7.

The phase centers of satellite antennas form a measurement basis moving in space (Fig. 8). There are 15 non-repeating bases in the polyhedron, some of which are internal. In fact, this is a complex case of the GNSS "Moving Base" mode, which allows to collection of a large statistical dataset for accuracy estimation of the functioning of multisystem, multifrequency satellite equipment in dynamics.

Before the experiments were performed, special preparation needed to be done. This preparation includes flight plan design and analysis of the meteorological conditions, such as cloudiness, visibility, wind speed, and direction. Eventually, an approximate flight route and altitude are planned. Based on that preparation, the resulting flight routes, projected on the earth surface, from experiments done on September 14 and December 16 of 2018 are shown in Fig. 9. The experiment was carried out at low air temperatures (− 22–25 °C). The installation of MAMS equipment on board the balloon is shown in Fig. 10.

Experiment results

The navigational data are obtained using GNSS and INS measurements. Data processing was done by NovAtel Waypoint Inertial Explorer software. The collected measurements were processed in the RTKLIB software for the experiment performed on September 14, 2018, and in the software RTKLIB and WayPoint Inertial Explorer for the experiment conducted on December 16, 2018 (Takasu and Yasuda 2009; Ferreira et al. 2020). For the last one, the data from the separately located inertial system SPAN-CPT6 was used. The altitude of the combined phase center of MAMS during flight is shown in Fig. 11. A multisystem smart antenna installed at the launch site was used as a relative reference base station.

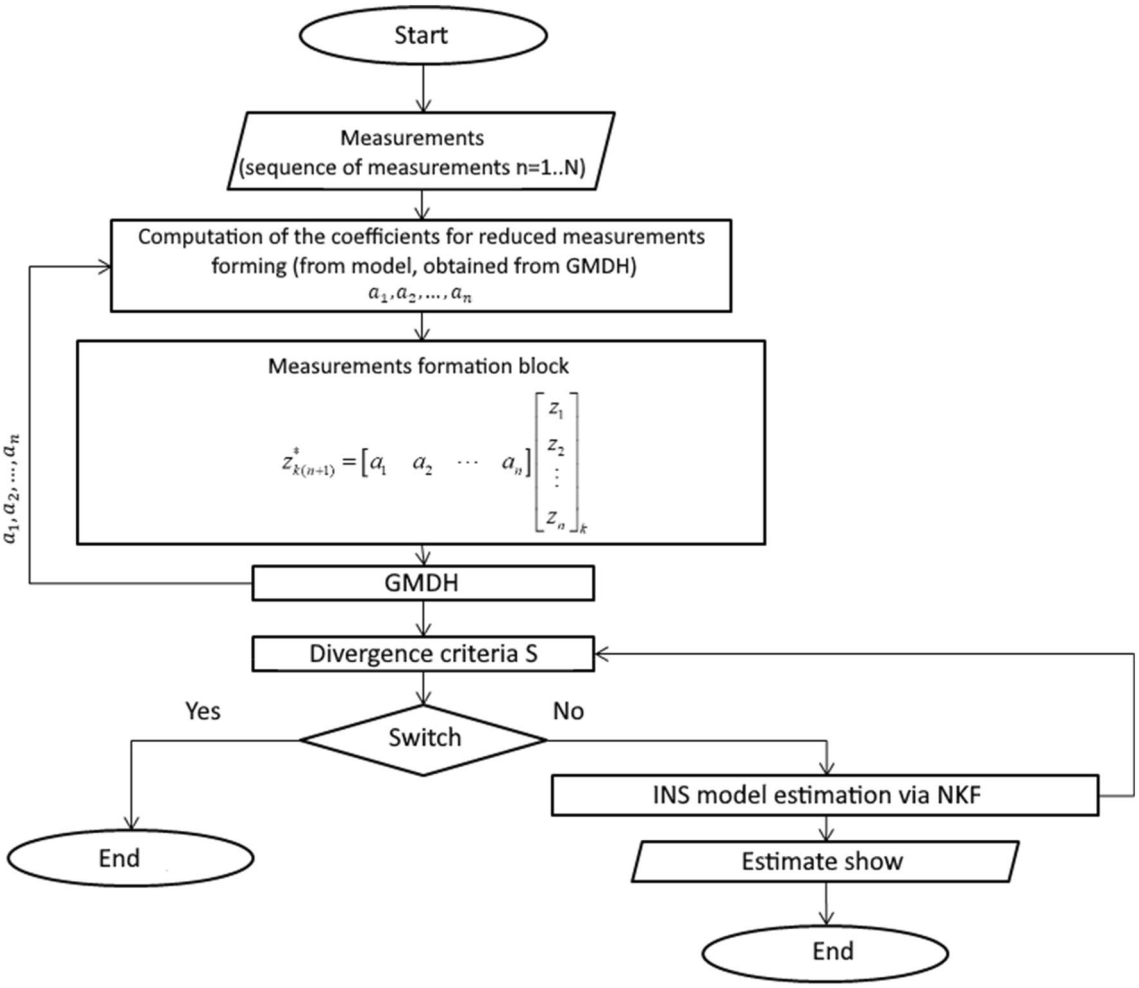

Fig. 4 Proposed adaptive NKF. The coefficients for the reduced measurements are computed using the obtained measurements. Then reduced measurements are computed, and the GMDH algorithm is applied. If the divergence criteria are satisfied, the process stops. If not satisfied, the INS model is additionally estimated via NKF

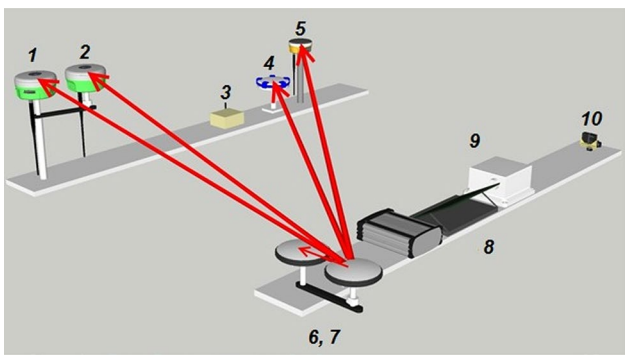

Fig. 5 MAMS schematic diagram. 1, 2 are the JSC PA UOMZ MP-8 and MP-10 smart antennas; 3, 4 are the AMSA-3 antennas with the base module; 5 is the UniStrongG970-II smart antenna (GNSS data up to 50 Hz); 6, 7 are the GNSS antennas NovAtelGG702-1.02; 8 is the MAMS control module; 9 is the inertial navigation system (INS) NovAtelSPAN-CPT6; 10 is the web camera for photo and video recording of the experiment

Fig. 6 MAMS pre-flight setup. Two GNSS antennas, GPStation-6 and SPAN-CPT are shown here. Additional Power supply via battery is also presented

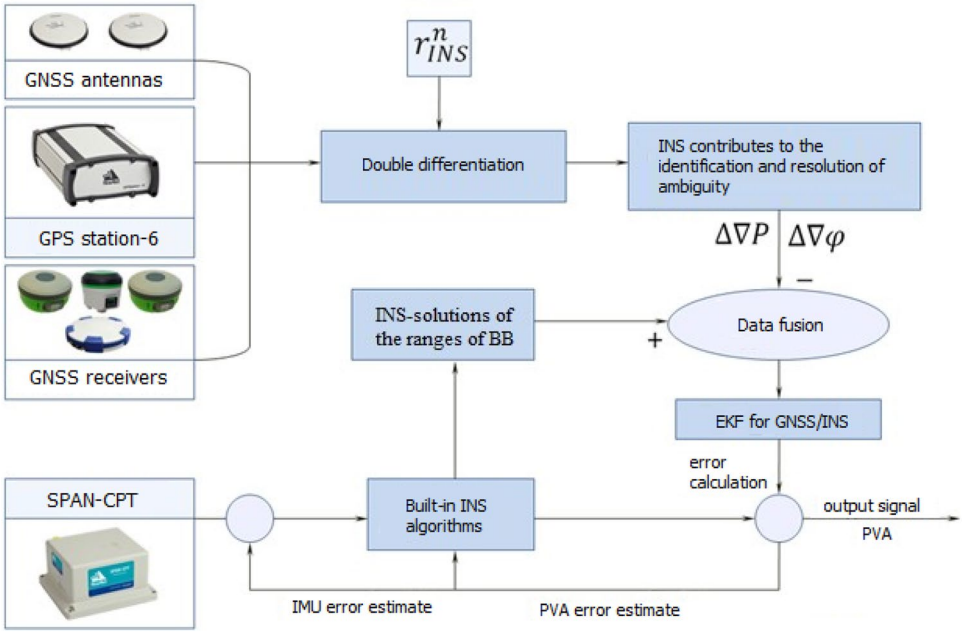

Fig. 7 General functional scheme of the MAMS complex. DD denotes double differences; EKF is the extended Kalman filter, and PVA is the position, velocity, and altitude

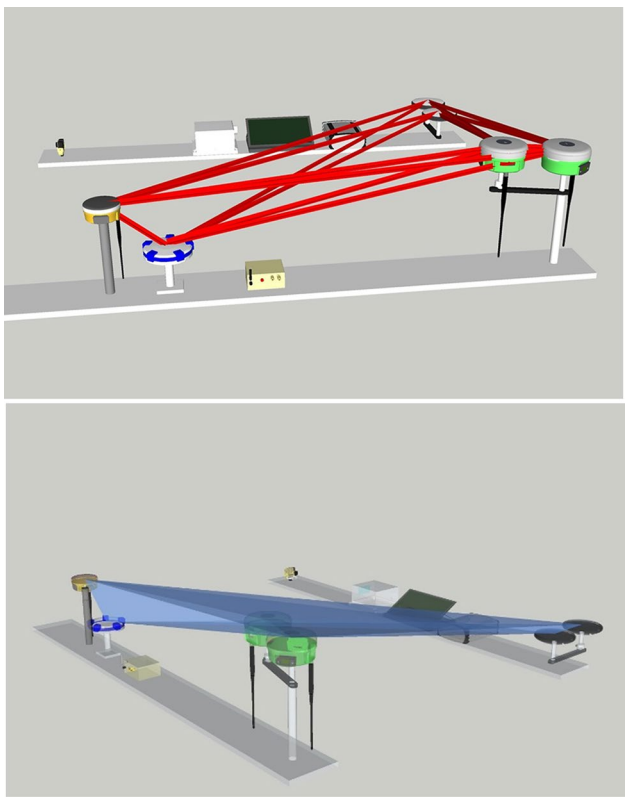

Fig. 8 Phase centers determined by the GNSS. Top: baselines determined by the GNSS antenna phase centers. Bottom: space-moving stereometric figures consisting of baselines determined by the GNSS antenna phase centers

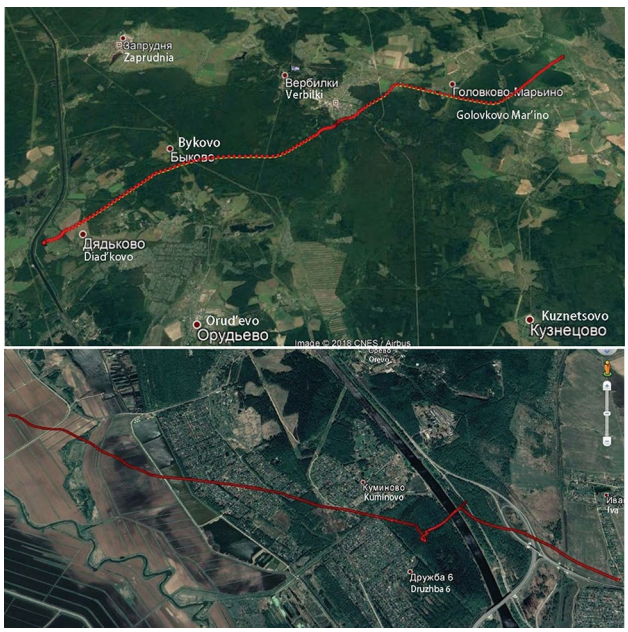

Fig. 9 Experimental Routes. Route of September 14, 2018 (top), and December 16, 2018 (bottom)

The balloon speed was also computed from the measured data set in the RTKLIB software and shown in Fig. 12. Velocities computed by processing inertial data in the InertialExplorer software are presented in Fig. 13. Accelerations computed from processing inertial data in the InertialExplorer software are shown in Fig. 14. The dynamics of the root mean square error obtained from processed inertial data in the InertialExplorer software is presented in Fig. 15.

Fig. 10 MAMS-fixed equipment MR-8 and MR-10 are shown at the top and additional GNSS antenna and computation module are shown at the bottom

The results of a full-scale experiment are shown in Figs. 16 and 17. The balloon keeps its spatial position in the absence of wind. Up to the time moment 1, the navigation complex operates as part of the INS; GNSS and adaptive NKF as illustrated in Fig. 16. At the period, defined between moment 1 and moment 2, there was no GNSS data, and only INS measurements are presented. As a result, the INS errors significantly increase, as illustrated in Figs. 16 and 17.

Those Figs. 16 and 17 illustrate change in balloon coordinates $(\Delta X, \Delta Y, \Delta Z)$ obtained as the output of the combined GNSS/INS system. After 40 s, the GNSS signal appears again, and the INS error model construction process is started using GMDH and adaptive NKF. Then this model is used in adaptive NKF to correct the navigational data. From moment 3 onward, the navigational data became satisfactory, meaning that the accuracy of determining coordinates became about 0.10 m. It took 45 s from moment 2 to achieve such accuracy.

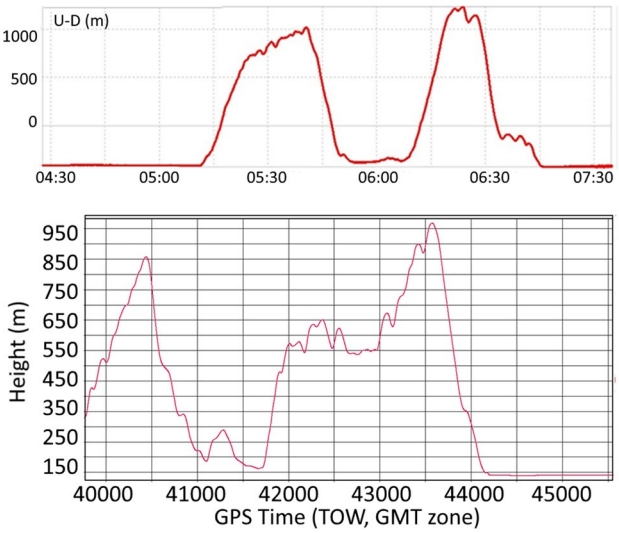

Fig. 11 Graph of the MAIS GNSS equipment combined phase center heights. The data obtained from the experiment on September 14, 2018 is shown on the top, and the data from the experiment at December 16, 2018 is shown at the bottom

Figure 15 illustrates the results obtained when the INS error model was constructed by GMDH with data from previous experiments for this particular INS. An adaptive NKF with this prepared model is used in the combined GNSS/INS system. Figure 17 presents results where the model is refined during the assessment process. Here GMDH is adjusting the initial model during the time from 60 to 65 s. It took 32 s to achieve desired positioning accuracy within 0.10 m from moment 2. Thus, using the INS error model constructed in advance, which is used in the adaptive NKF, reduces the time required for the navigation complex to enter the normal operating mode. The INS estimation error with this model is shown in Fig. 16 as line 2.

The model constructed by GMDH algorithm from the measurements, which is formed from 40 s, has the form:

$$y_1(\delta x) = b_{01} + b_{11}x_1 + b_{21}x_3 + b_{31}x_1^2 + b_{41}x_3^2 + b_{51}x_1x_3$$

$$b_{01} = 0.52,\ b_{11} = -1.13,\ b_{21} = 86.34,\ \ b_{31} = 1.02,$$

where $b_{41} = 0.007,$ and $b_{51} = -0.201.$

Using the INS error model constructed by GMDH within the two ways of NKF realization demonstrated good estimation accuracy. An exception is line 2 shown in Fig. 16 where the adaptive NKF is used. The INS errors model is somewhat different from the real INS errors; therefore, it is necessary to adjust the model during the operation of the INS. The second method of NKF implementation cannot perform model adjustments during its operation; therefore, it showed an accuracy of 15% worse.

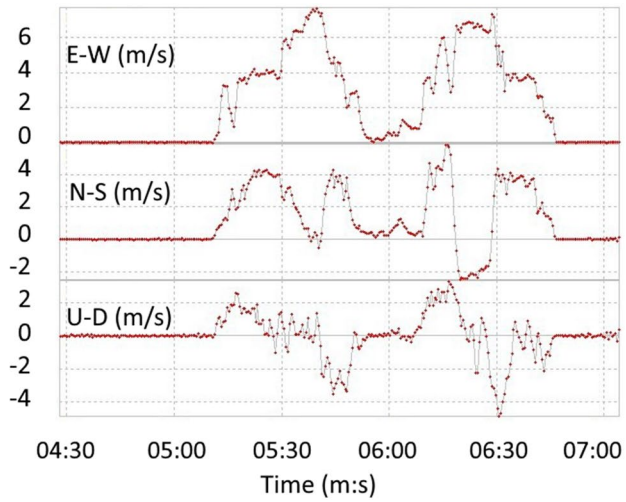

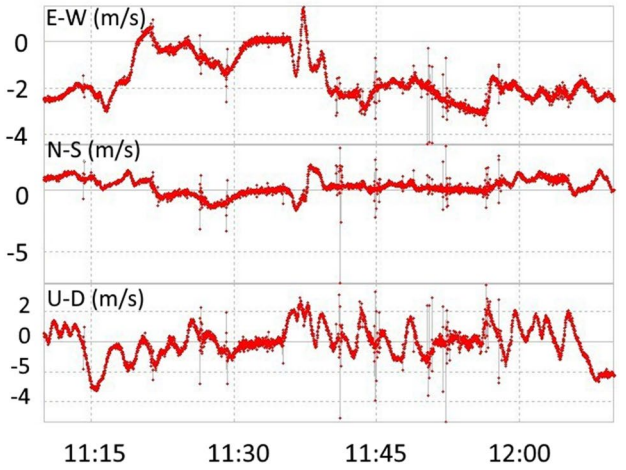

Fig. 12 Velocities obtained after data processing. Velocities obtained on September 14, 2018 (top), and December 16, 2018 (bottom). E–W, N–S, and U–D are the velocities in east–west, north–south, and Up–Down directions in units of m/s. Some outliers in velocity plots are also presented

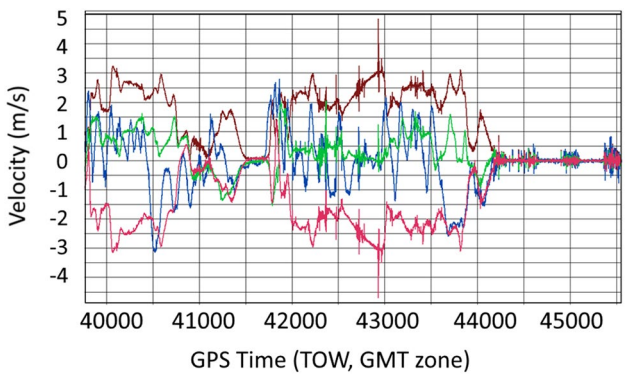

Fig. 13 Velocities obtained after the processing the data with InertialExplorer. Red line: east direction, green line: north direction, blue line: up direction, and brown line: horizontal speed

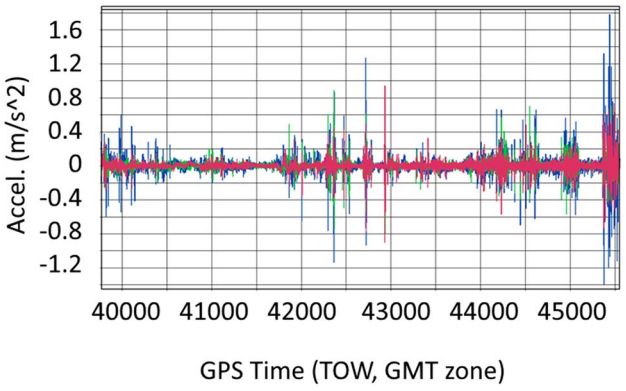

Fig. 14 Accelerations obtained after data processing with InertialExplorer. Red line: east direction, green line: north direction, blue line: up direction

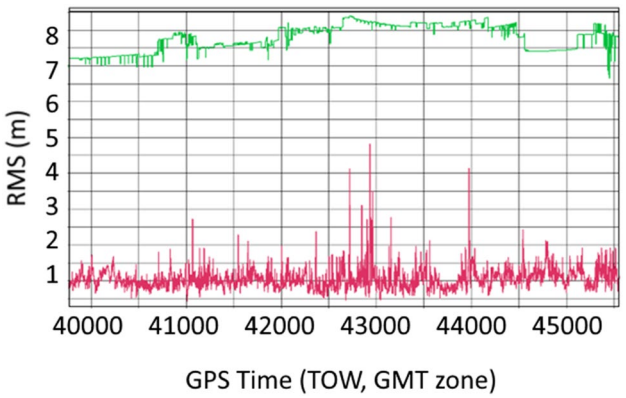

Fig. 15 RMS changing in InertialExplorer. Red line: RMS value. green line: standard deviation

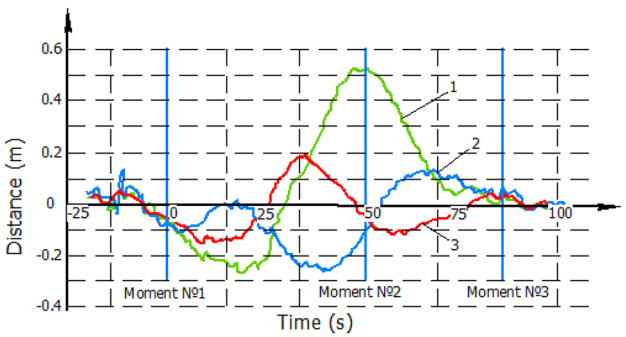

Fig. 16 Results of a full-scale experiment. Lines 1, 2, and 3 denotes INS errors in X, Y, and Z coordinates respectively. Three vertical lines added to highlight the time moments, where the behavior of the combined GNSS/INS is changed

We made the onboard tests with different correction approaches to compare numerical effectiveness and INS correction accuracy. The results of these tests are

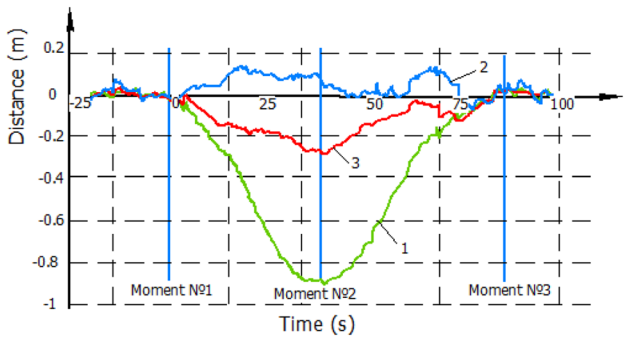

Fig. 17 Results of a full-scale experiment with GMDH. Lines 1, 2, and 3 denotes INS errors in X, Y, and Z coordinates respectively. Three vertical lines added to highlight the time moments, where the behavior of the combined GNSS/INS is changed

Table 1 Accuracy and numerical effectiveness of the proposed approach. NFK + GMDH is the proposed correction approach

Algorithm	Correction accuracy	Required RAM amount
NFK	81%	150 Kb
NFK + GMDH	90%	750 Kb
NFK + GA	92%	~7 Mb

NFK + GA is the correction approach where the genetic algorithm is used, and accuracy is computed in percent relative to INS error

presented in Table 1. INS correction accuracy with the proposed adaptive NKF modification is slightly higher than just NKF and almost equal to the approach where NKF is combined with a genetic algorithm for model construction. However, the required RAM amount for the proposed correction approach is significantly lower than the one with the genetic algorithm.

Conclusions and discussions

An INS algorithmic correction by GNSS data using an adaptive NKF is considered in this research. To increase the accuracy of the navigational data, the INS error model is used for correction in adaptive NKF. We proposed the INS/GNSS correction scheme via adaptive NKF with the measurement formation procedure and criterion of the estimation process divergence. The adaptive NKF uses the INS error model obtained from GMDH during the pre-flight test for a particular INS. The INS error model computed by the GMDH algorithm during flight highly depends on aircraft maneuvers and requires consistently constructing a new INS error model. The proposed idea to use the pre-built INS error model from pre-flight test results is to decrease the number of calculations that have to be done on the onboard computer. Using the INS error model obtained via GMDH compared to the classical INS error model increases the accuracy of the resulting navigational data. This is possible because GMDH could consider the specific features of a particular INS in the model.

The effectiveness of the proposed algorithmic solutions is proved by the data obtained from two flight experiments. The results of the flight experiments showed a reduction in the time for the combined GNSS/INS system to enter the normal operating mode when using a pre-built INS error model in the adaptive NKF.

Funding Ministry of Education and Science, #0705-2020-0041, Konstantin Neusypin

Data availability The obtained during the experiments data sets were not published and not available online but could be provided upon request.

References

Ali J, Jiancheng F (2005) SINS/ANS/GPS integration using federated Kalman filter based on optimized information-sharing coefficients. In: AIAA Guidance, navigation, and control conference and exhibit, San Francisco, USA, 6452

Belavkin RV (2013) Minimum of information distance criterion for optimal control of mutation rate in evolutionary systems. InQuantum Bio-Informatics, pp 95–115

Carvalho H, Del Moral P, Monin A, Salut G (1997) Optimal nonlinear filtering in GPS/INS integration. IEEE Trans Aerosp Electron Syst 3(33):835–850

Chechkin A, Pavlyukevich I (2014) Marcus versus Stratonovich for systems with jump noise. J Phys a: Math Theor 47(34):342001

Csorgo M, Dawson DA, Rao JNK, Saleh AME (1981) Statistics and related topics, 1st edn. North-Holland, Amsterdam, Netherlands, p 253

Fantinutto R, Guglieri G, Quagliotti FB (2005) Flight control system design and optimization with a genetic algorithm. Aerosp Sci Technol 9(1):73–80

Ferreira A, Matias B, Almeida J, Silva E (2020) Real-time GNSS precise positioning: RTKLIB for ROS. Int J Adv Rob Syst 17:1–8. https://doi.org/10.1177/1729881420904526

Gao S, Feng Z, Li H (2006) Random weighting estimation of white noise error characteristic in integrated INS/GPS/SAR system. In: 2006 International Conference on Computational Intelligence for Modelling Control and Automation and International Conference on Intelligent Agents Web Technologies and International Commerce (CIMCA'06), IEEE

George M, Sukkarieh S (2005) Tightly coupled INS/GPS with bias estimation for UAV applications. In: Proceedings of Australasian Conference on Robotics and Automation (ACRA), Sydney, Australia

Ivakhnenko AG (1970) Heuristic self-organization in problems of engineering cybernetics. Automatica 6(2):207–219

Ivakhnenko AG (1971) Polynomial theory of complex systems. IEEE Trans Syst, Man and Cybern. SMC 1(4):364–378

Julier SJ, Uhlmann JK (1997) A new extension of the Kalman filter to nonlinear systems. Def Sens, Simul Controls 3068:182–193

Kondo T (1998) GMDH neural network algorithm using the heuristic self-organization method and its application to the pattern

identification problem. In: Proceedings of the 37th SICE Annual Conference. International Session Papers, Tokyo, Japan, pp. 1143–1148
Kurtz TG, Pardoux É, Protter P (1995) Stratonovich stochastic differential equations driven by general semimartingales. Annales De l'IHP Probabilités Et Statistique 31(2):351–377
Lee JH, Ricker NL (1994) Extended Kalman filter based nonlinear model predictive control. Ind Eng Chem Res 33(6):1530–1541
Neusypin KA, Selezneva MS, Tsibizova TY (2018) Diagnostics algorithms for flight vehicles navigation complex. In: 2018 International Russian Automation Conference (RusAutoCon), Sochi, Russia, 16–23 September 2018, pp. 1–6
Proletarsky AV, Neusypin KA, Selezneva MS (2019) Method for improving accuracy of INS using scalar parametric identification. In: International Russian Automation Conference (RusAutoCon), Chelyabinsk, Russia, September 8–14, pp. 1–4
Rao JNK (1980) Estimating the common mean of possibly different normal populations: a simulation study. J Am Stat Assoc 75(370):447–453
Selezneva MS, Neusypin KA (2016) Development of a measurement complex with intelligent component. Meas Tech 59(9):916–922
Selezneva MS, Neusypin KA, Proletarsky AV (2017) Novel variable structure measurement system with intelligent components for flight vehicles. Metrol Measurement Syst 24(2):347–356
Selezneva MS, Proletarsky AV, Neusypin KA, Lifei Z (2019) Modification of the federated Kalman filter using the observability degree criterion of state variables. In: 26th Saint Petersburg International Conference on Integrated Navigation Systems (ICINS), Saint Petersburg, Russia, May 27–29, pp. 1–3
Shen K, Proletarsky AV, Neusypin KA (2016) Algorithms of constructing models for compensating navigation systems of unmanned aerial vehicles. In: 2016 International Conference on Robotics and Automation Engineering (ICRAE), Stockholm, Sweden, pp. 104–108
Šimandl M, Královec J, Tichavský P (2001) Filtering, predictive, and smoothing Cramér–Rao bounds for discrete-time nonlinear dynamic systems. Automatica 37(11):1703–1716
Simon DT (2006) Using nonlinear Kalman filtering to estimate signals. Embedded Syst Des 19(7):38
Song S, Wang L (2017) Modified GMDH-NN algorithm and its application for global sensitivity analysis. J Comput Phys 348:534–548
Takasu T, Yasuda A (2009) Development of the low-cost RTK-GPS receiver with an open source program package RTKLIB. In: Proceedings of the International symposium on GPS/GNSS, Jeju, Korea. pp 4–6
Tichavsky P, Muravchik CH, Nehorai A (1998) Posterior Cramér–Rao bounds for discrete-time nonlinear filtering. IEEE Trans Signal Process 46(5):1386–1396
Trees HLV, Bell KL (2007) Bayesian bounds for parameter estimation and nonlinear filtering/tracking, 1st edn. Wiley-IEEE press, New York
Wan EA, Nelson A (2001) Dual extended Kalman filter methods. In: Haykin S (ed) Kalman filtering and neural networks. Wiley, New York, pp 123–174
Yang Y, Liu X, Zhang W, Liu X, Guo Y (2020) A nonlinear double model for multisensor-integrated navigation using the federated EKF algorithm for small UAVs. Sensors 20(10):2974
Yin Y, Song C, Li M, Niu Q (2019) A CSI-based indoor fingerprinting localization with model integration approach. Sensors 19(13):2998
Zheng B, Fu P, Li B, Yuan X (2018) A robust adaptive unscented Kalman filter for nonlinear estimation with uncertain noise covariance. Sensors 18(3):808

Konstantin Neusypin Received his D.Sc. in 1996. He is a laureate of the Russian Government Award and is a Professor and Chair of the Automatic Control Systems Department at Bauman Moscow State Technical University. Research interests include problems of correction algorithms of the navigation complexes.

Andrey Kupriyanov Received his Ph.D. in 1976. Research interests include high-precision GNSS measurements. He is a member of Group C at the International Committee on Global Navigation Satellite Systems (ICG) at the United Nations Office for Outer Space Affairs (UNOOSA). He is an Associate Professor and Dep. Chair of the Applied Geodesy Dept. at Moscow State University of Geodesy and Cartography.

Andrey Maslennikov Received his M.Sc. in 2013 and an Engineering degree in 2014. He is a Senior Lecturer at the Automatic Control Systems Dept. at Bauman Moscow State Technical University, with research interests in algorithms for the correction and fusion of GNSS data.

Maria Selezneva Received her Ph.D. in 2017. She is a laureate of the Russian Government Award and Associate Professor and Dep. Chair of the Automatic Control Systems Dept. at Bauman Moscow State Technical University. Research interests include algorithms for fusion in measurement systems.